PHENOMENOLOGY OF LIGHT STERILE NEUTRINOS*

C. Giunti

INFN, Sezione di Torino, Via P. Giuria 1, 10125 Torino, Italy

(Received January 25, 2013)

I review the analysis of ν_e and $\bar{\nu}_e$ disappearance experiments in terms of neutrino oscillations in the framework of 3+1 neutrino mixing.

DOI:10.5506/APhysPolBSupp.6.667
PACS numbers: 14.60.Pq, 14.60.Lm, 14.60.St

1. Introduction

Neutrino physics experienced in 1998 a wonderful success with the Super-Kamiokande measurement of the up–down asymmetry of high-energy atmospheric ν_μs, which gave a model-independent proof of atmospheric neutrino oscillations. A few years later, the measurement of neutral-current and charged-current solar neutrino events in the SNO experiment gave a model-independent proof of the oscillations of solar ν_es. These oscillations, which have been confirmed in the last decade by several long-baseline experiments, are nicely explained in the framework of three-neutrino mixing, which is the current paradigm of neutrino physics (see [1]). However, several short-baseline neutrino oscillation experiments found signals which may be due to neutrino oscillations beyond the three-neutrino mixing paradigm, with mixing of the three active neutrinos ν_e, ν_μ, ν_τ with sterile neutrinos (see [1]).

In this review, I consider the gallium anomaly [2, 3] and the reactor anomaly [4–6], which indicate that electron neutrino and antineutrinos may disappear at short distances (see [3]). Such disappearance can be explained by the presence of at least one massive neutrino at the eV scale, such that its squared-mass difference with the three ordinary massive neutrinos is much larger than the squared-mass differences operating in solar, atmospheric and

* Presented at the International Symposium on Multiparticle Dynamics, Kielce, Poland, September 17–21, 2012.

long-baseline neutrino oscillation experiments. Since from the LEP measurement of the invisible width of the Z boson we know that there are only three light active flavor neutrinos, in the flavor basis the additional neutrinos are sterile.

Another very interesting indication on favor of short-baseline oscillations generated by the existence of light sterile neutrinos is the LSND $\bar{\nu}_\mu \to \nu_e$ signal. However, this indication is more controversial, because it is in tension with the results of short-baseline $\overset{(-)}{\nu}_e$ and $\overset{(-)}{\nu}_\mu$ disappearance experiments (see [1]) and because it has not been either confirmed or confuted by the recent MiniBooNE experiment.

In this review, I discuss the indications in favor of short-baseline ν_e and $\bar{\nu}_e$ disappearance in the framework of 3+1 neutrino mixing. The mixing of the three active flavor neutrino fields ν_e, ν_μ, ν_τ and one sterile neutrino field ν_s is given by

$$\nu_\alpha = \sum_{k=1}^{4} U_{\alpha k} \nu_k \qquad (\alpha = e, \mu, \tau, s)\,, \tag{1}$$

where U is the unitary 4×4 mixing matrix ($U^\dagger = U^{-1}$) and each of the four ν_ks is a massive neutrino field with mass m_k. The neutrino squared-mass differences are assumed to satisfy the hierarchy

$$\Delta m^2_{21} \ll \Delta m^2_{31} \ll \Delta m^2_{41}\,, \tag{2}$$

with $\Delta m^2_{kj} \equiv m^2_k - m^2_j$, such that Δm^2_{21} generates solar neutrino oscillations, Δm^2_{31} generates atmospheric neutrino oscillations, and Δm^2_{41} generates short-baseline oscillations.

The effective survival probability at a distance L of electron neutrinos and antineutrinos with energy E in short-baseline neutrino oscillation experiments is given by (see [1])

$$P^{\text{SBL}}_{\substack{(-)\ (-)\\ \nu_e \to \nu_e}} = 1 - \sin^2 2\vartheta_{ee} \sin^2 \left(\frac{\Delta m^2_{41} L}{4E} \right)\,, \tag{3}$$

with the transition amplitude

$$\sin^2 2\vartheta_{ee} = 4 |U_{e4}|^2 \left(1 - |U_{e4}|^2 \right)\,. \tag{4}$$

2. Gallium anomaly

The GALLEX and SAGE gallium solar neutrino experiments have been tested with intense artificial ^{51}Cr and ^{37}Ar radioactive sources which produce electron neutrinos through electron capture with energies (branching ratios)

$$E\left(^{51}\text{Cr}\right) = 747\,(81.63\%),\ 752\,(8.49\%),\ 427\,(8.95\%),\ 432\,(0.93\%)\,\text{keV}\,, \tag{5}$$

$$E\left(^{37}\text{Ar}\right) = 811\,(90.2\%),\ 813\,(09.8\%)\,\text{keV}\,. \tag{6}$$

In each of these experiments, the source was placed near the center of the approximately cylindrical detector and electron neutrinos have been detected with the solar neutrino detection reaction

$$\nu_e + {}^{71}\mathrm{Ga} \to {}^{71}\mathrm{Ge} + e^- \,. \tag{7}$$

The average neutrino traveling distances are $\langle L\rangle_{\mathrm{GALLEX}} = 1.9\,\mathrm{m}$ and $\langle L\rangle_{\mathrm{SAGE}} = 0.6\,\mathrm{m}$. The ratios R_{B} of measured and expected ^{71}Ge event rates reported by the experimental collaborations are

$$R_{\mathrm{B}}^{\mathrm{G1}} = 0.95^{+0.11}_{-0.11}\,, \quad R_{\mathrm{B}}^{\mathrm{G2}} = 0.81^{+0.10}_{-0.11}\,, \quad R_{\mathrm{B}}^{\mathrm{S1}} = 0.95^{+0.12}_{-0.12}\,, \quad R_{\mathrm{B}}^{\mathrm{S2}} = 0.79^{+0.08}_{-0.08}\,. \tag{8}$$

G1 and G2 denote the two GALLEX experiments with ^{51}Cr sources, S1 denotes the SAGE experiment with a ^{51}Cr source, and S2 denotes the SAGE experiment with a ^{37}Ar source. The index B indicates that the expected event rates have been calculated using the Bahcall cross sections [7]

$$\sigma_{\mathrm{B}}\left({}^{51}\mathrm{Cr}\right) = 58.1 \times 10^{-46}\,\mathrm{cm}^2\,, \qquad \sigma_{\mathrm{B}}\left({}^{37}\mathrm{Ar}\right) = 70.0 \times 10^{-46}\,\mathrm{cm}^2\,, \tag{9}$$

without considering their uncertainties. One can see that the values of $R_{\mathrm{B}}^{\mathrm{G1}}$ and $R_{\mathrm{B}}^{\mathrm{S1}}$ indicate a compatibility between the measured and expected event rates, whereas the values of $R_{\mathrm{B}}^{\mathrm{G2}}$ and $R_{\mathrm{B}}^{\mathrm{S2}}$ are significantly smaller than one, indicating a disappearance of electron neutrinos. The weighted average

$$R_{\mathrm{B}} = 0.86^{+0.05}_{-0.05} \tag{10}$$

gives a 2.7σ anomaly.

Since the values of the cross sections of ^{51}Cr and ^{37}Ar electron neutrinos and their uncertainties are crucial for the interpretation of the gallium data as indication of short-baseline ν_e disappearance, in the following, I discuss in detail the problem of the determination of the cross sections and their uncertainties, taking into account [7–9] and the important recent measurement in [10].

The cross sections of the interaction process (7) for neutrinos produced by ^{51}Cr and ^{37}Ar sources are given by

$$\sigma = \sigma_{\mathrm{gs}}\left(1 + \xi_{175}\frac{\mathrm{BGT}_{175}}{\mathrm{BGT}_{\mathrm{gs}}} + \xi_{500}\frac{\mathrm{BGT}_{500}}{\mathrm{BGT}_{\mathrm{gs}}}\right)\,, \tag{11}$$

where σ_{gs} is the cross sections of the transitions from the ground state of ^{71}Ga to the ground state of ^{71}Ge, $\mathrm{BGT}_{\mathrm{gs}}$ is the corresponding Gamow–Teller strength, and BGT_{175} and BGT_{500} are the Gamow–Teller strengths of the transitions from the ground state of ^{71}Ga to the two excited states of ^{71}Ge at about 175 keV and 500 keV (see Fig. 1 (a)). The coefficients

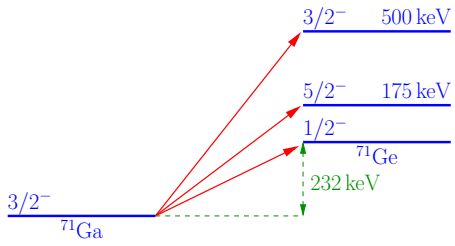

(a)

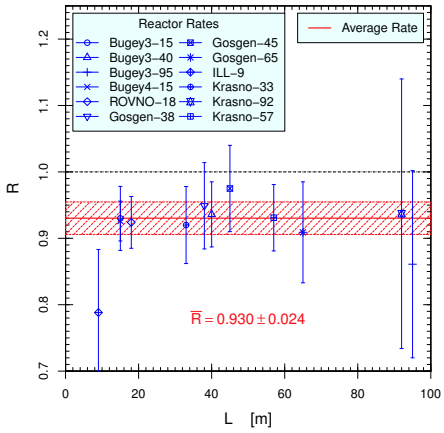

(b)

Fig. 1. (a) ^{71}Ga $\to^{71}$ Ge transitions induced by ^{51}Cr and ^{37}Ar electron neutrinos [3]. (b) Ratio R of the observed $\bar{\nu}_e$ event rate and that expected in absence of $\bar{\nu}_e$ disappearance in reactor neutrino experiments [3]. The horizontal band represents the average value of R with 1σ uncertainties.

of $\mathrm{BGT}_{175}/\mathrm{BGT}_{\mathrm{gs}}$ and $\mathrm{BGT}_{500}/\mathrm{BGT}_{\mathrm{gs}}$ are determined by phase space: $\xi_{175}(^{51}\mathrm{Cr}) = 0.669$, $\xi_{500}(^{51}\mathrm{Cr}) = 0.220$, $\xi_{175}(^{37}\mathrm{Ar}) = 0.695$, $\xi_{500}(^{37}\mathrm{Ar}) = 0.263$ [7].

The cross sections of the transitions from the ground state of ^{71}Ga to the ground state of ^{71}Ge have been calculated accurately by Bahcall [7]

$$\sigma_{\mathrm{gs}}\left(^{51}\mathrm{Cr}\right) = 55.3 \times 10^{-46}\,\mathrm{cm}^2\,, \qquad \sigma_{\mathrm{gs}}\left(^{37}\mathrm{Ar}\right) = 66.2 \times 10^{-46}\,\mathrm{cm}^2\,. \quad (12)$$

These cross sections are proportional to the characteristic neutrino absorption cross section [7]

$$\sigma_0 = 2\alpha Z_{\mathrm{Ge}} m_e^2 G_{\mathrm{F}}^2 |V_{ud}|^2 g_A^2 \mathrm{BGT}_{\mathrm{gs}} = Z_{\mathrm{Ge}} \mathrm{BGT}_{\mathrm{gs}} (3.091 \pm 0.012) \times 10^{-46}\,\mathrm{cm}^2\,, \quad (13)$$

where α is the fine-structure constant, $Z_{\mathrm{Ge}} = 32$ is the atomic number of the final nucleus, m_e is the electron mass, G_{F} is the Fermi constant, V_{ud} is the ud element of the quark mixing matrix V, and g_{A} is the axial coupling constant. The numerical value of the coefficient in the last line of Eq. (13) has been obtained with the values of these quantities given in the 2012 Review of Particle Physics. From the value

$$\sigma_0 = (8.611 \pm 0.011) \times 10^{-46}\,\mathrm{cm}^2\,, \quad (14)$$

calculated by Bahcall [7] using the accurate measurement [11]

$$T_{1/2}\left(^{71}\mathrm{Ge}\right) = 11.43 \pm 0.03\,\mathrm{d} \quad (15)$$

of the lifetime of ^{71}Ge (which decays through the electron-capture process $e^- + {}^{71}_{32}\mathrm{Ge} \to {}^{71}_{31}\mathrm{Ga} + \nu_e$, which is the inverse of the ν_e detection process (7)), we obtain

$$\mathrm{BGT}_{\mathrm{gs}} = 0.0871 \pm 0.0004\,. \tag{16}$$

The Gamow–Teller strengths BGT_{175} and BGT_{500} have been measured in 1985 in the (p,n) experiment of Krofcheck *et al.* [8] and recently, in 2011, in the (^{3}He,^{3}H) experiment of Frekers *et al.* [10]. The results are listed in Table I together with the 1998 shell-model calculation of BGT_{175} of Haxton [9].

TABLE I

Gamow–Teller strengths of the transitions from the ground state of ^{71}Ga to the two excited states of ^{71}Ge at 175 keV and 500 keV obtained by Krofcheck *et al.* [8], Haxton [9] and Frekers *et al.* [10].

Reference	Method	BGT_{175}	BGT_{500}
Krofcheck *et al.*	$^{71}\mathrm{Ga}(p,n)^{71}\mathrm{Ge}$	< 0.005	0.011 ± 0.002
Haxton	Shell Model	0.017 ± 0.015	
Frekers *et al.*	$^{71}\mathrm{Ga}(^3\mathrm{He},^3\mathrm{H})^{71}\mathrm{Ge}$	0.0034 ± 0.0026	0.0176 ± 0.0014

The Bahcall cross sections (9) have been obtained using for BGT_{500} the Krofcheck *et al.* [8] measurement and for BGT_{175} half of the Krofcheck *et al.* upper limit [7].

The authors of [2] used the Haxton shell-model value of BGT_{175} and the (p,n) measured value of BGT_{500}. Although the uncertainties of the Haxton shell-model value of BGT_{175} are so large that BGT_{175} may be negligibly small, the central value is much larger than the upper limit obtained in the (p,n) experiment. According to [9], this is due to a suppression of the (p,n) value caused by a destructive interference between the spin ($\Delta J = 1$, $\Delta L = 0$) matrix element and an additional spin-tensor ($\Delta J = 1$, $\Delta L = 2$) matrix element which operates only in (p,n) transitions. We do not know if the same suppression is operating also in (^{3}He,^{3}H), which could be the explanation of the smallness of the value of BGT_{175} measured by Frekers *et al.* [10], which is compatible with the (p,n) upper bound. Moreover, the value of BGT_{500} measured by Frekers *et al.* [10] has a 2.7σ discrepancy with that measured by Krofcheck *et al.* [8]. Hence, the authors of [3] considered three different combinations of the two Gamow–Teller strengths: (HK) Haxton BGT_{175} value and Krofcheck *et al.* [8] BGT_{500} value; (FF) Frekers *et al.* [10] values of both BGT_{175} and BGT_{500}; (HF) Haxton BGT_{175} value and Frekers *et al.* [10] BGT_{500} value. The corresponding weighted averages of measured and expected ^{71}Ge event rates are

$$R_{\mathrm{HK}} = 0.77^{+0.08}_{-0.08}\,, \qquad R_{\mathrm{FF}} = 0.84^{+0.05}_{-0.05}\,, \qquad R_{\mathrm{HF}} = 0.75^{+0.09}_{-0.07}\,. \tag{17}$$

Since the statistical significance of the gallium anomaly in the three cases is, respectively, about 3.0σ, 2.9σ and 3.1σ, the new (^{3}He,^{3} H) cross section measurement of Frekers *et al.* [10] confirms that there is a gallium anomaly at a level of about 3σ [2], which indicates a short-baseline disappearance of ν_e which can be explained by neutrino oscillations.

3. Fit of gallium and reactor data

The reactor antineutrino anomaly [5] stems from a new evaluation of the reactor $\bar{\nu}_e$ flux [4, 6] which implies that the event rate measured by several reactor $\bar{\nu}_e$ experiments at distances from the reactor core between about 10 and 100 meters is smaller than that obtained without $\bar{\nu}_e$ disappearance. This is illustrated in Fig. 1 (b) taken from [3], which shows the ratio R of the observed $\bar{\nu}_e$ event rate and that expected in absence of $\bar{\nu}_e$ disappearance for the Bugey-3, Bugey-4, ROVNO91, Gosgen, ILL and Krasnoyarsk reactor antineutrino experiments (see [3]). The reactor neutrino fluxes are taken from the recent White Paper on light sterile neutrinos [12], which updates [4–6]. From Fig. 1 (b), one can see that the reactor antineutrino anomaly has a significance of about 2.8σ. In the fit of reactor data, besides the above-mentioned rates, the authors of [3] considered also the 40 m/15 m spectral ratio measured in the Bugey-3 experiment.

In [3], it has been shown that when combined with the reactor data, the gallium data in the three cases discussed above give similar results for the allowed values of the oscillation parameters $\sin^2 2\vartheta_{ee}$ and Δm^2_{41}. Hence, in the following, I consider only the FF case, for which the best fit with $\chi^2_{\text{min}} = 31.8$ for 40 degrees of freedom is achieved for $\sin^2 2\vartheta_{ee} = 0.16$ and $\Delta m^2_{41} = 1.95\,\text{eV}^2$.

4. Global fit

Besides the gallium and reactor anomalies, in a global fit of electron neutrino and antineutrino disappearance data one must consider also the solar neutrino constraint on $\sin^2 2\vartheta_{ee}$ (see [3]) and the KARMEN and LSND $\nu_e + {}^{12}\text{C} \to {}^{12}\text{N}_{\text{gs}} + e^-$ scattering data (see [13]).

Figure 2 (a) shows a comparison of the allowed 95% C.L. regions in the $\sin^2 2\vartheta_{ee}$–Δm^2_{41} plane obtained from the separate fits of gallium, reactor, solar and ν_eC scattering data and from the combined fit of all data. One can see that the separate allowed regions overlap in a band delimited by $\Delta m^2_{41} \gtrsim 1\,\text{eV}^2$ and $0.07 \lesssim \sin^2 2\vartheta_{ee} \lesssim 0.09$, which is included in the globally allowed 95% C.L. region. Figure 2 (b) shows the globally allowed regions in the $\sin^2 2\vartheta_{ee}$–Δm^2_{41} plane and the marginal $\Delta\chi^2$s for the two oscillation

parameters. The best-fit point is at a relatively large value of Δm^2_{41},

$$\left(\Delta m^2_{41}\right)_{\rm bf} = 7.6\,{\rm eV}^2\,, \qquad \left(\sin^2 2\vartheta_{ee}\right)_{\rm bf} = 0.12\,, \tag{18}$$

with $\chi^2_{\rm min}/{\rm NDF} = 45.5/51$, corresponding to a 69% goodness-of-fit. However, there is a region allowed at 1σ around $\Delta m^2_{41} \simeq 2\,{\rm eV}^2$ and $\sin^2 2\vartheta_{ee} \simeq 0.1$. The slight preference of the global fit for $\Delta m^2_{41} \simeq 7.6\,{\rm eV}^2$ with respect to $\Delta m^2_{41} \simeq 2\,{\rm eV}^2$ (see the marginal $\Delta\chi^2$ for Δm^2_{41} in Fig. 2 (b)), which is preferred by gallium and reactor data, is due to the ν_eC scattering data, which prefer larger values of Δm^2_{41} (see [13]).

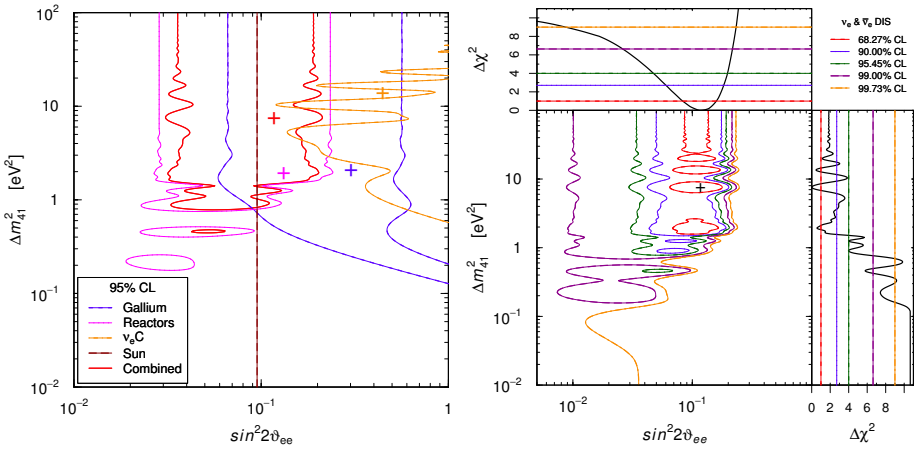

(a) (b)

Fig. 2. (a) Allowed 95% C.L. regions in the $\sin^2 2\vartheta_{ee}$–Δm^2_{41} plane obtained from the separate fits of gallium, reactor, solar and ν_eC scattering data and from the combined fit of all data [3]. The best-fit points corresponding to $\chi^2_{\rm min}$ are indicated by crosses. (b) Allowed regions in the $\sin^2 2\vartheta_{ee}$–Δm^2_{41} plane and marginal $\Delta\chi^2$s for $\sin^2 2\vartheta_{ee}$ and Δm^2_{41} obtained from the global fit of ν_e and $\bar{\nu}_e$ data. The best-fit point corresponding to $\chi^2_{\rm min}$ is indicated by a cross.

Comparing the minimum of the χ^2 of the global fit with the sum of the minima of the χ^2 of the separate fits of gallium, reactor, solar and ν_eC scattering data, we obtained $\Delta\chi^2_{\rm PG} = 11.5$, with 5 degrees of freedom, which gives a parameter goodness-of-fit of 4%. Therefore, the compatibility of the four data sets is acceptable.

The results of the global fit, as well as the results of the fits of gallium and reactor data, lead to lower limits for Δm^2_{41}, but there is no upper limit for Δm^2_{41} in Fig. 2 (b). Hence, one can ask if there are other measurements which constrain large values of Δm^2_{41}. The answer is positive and comes from the measurements of the effects of heavy neutrino masses on electron

spectrum in β-decay far from the end-point, from the results of neutrinoless double-β decay experiments for Majorana neutrinos, and from cosmological measurements (see [3, 14]).

5. Conclusions

The gallium and reactor neutrino anomalies indicate that ν_e and $\bar{\nu}_e$ disappear at short distances. This disappearance can be due to neutrino oscillations in the simplest 3+1 extension of the standard three-neutrino mixing paradigm which explains the well-measured oscillations of neutrinos in solar, atmospheric and long-baseline experiments. In the flavor basis, the additional neutrino is sterile. The corresponding massive neutrino has a mass larger than about 1 eV.

Since the proof of the existence of sterile neutrinos would be a very important information on the physics beyond the Standard Model and a neutrino mass at the eV scale would allow several experimentally accessible measurements, many projects aimed at checking the gallium and reactor anomalies with electron neutrino and antineutrino radioactive sources reactor electron antineutrinos and accelerator electron neutrinos have been proposed (see [12]). Thus, it is likely that in a few years we will know if the sterile neutrinos connected with these anomalies exist or not.

REFERENCES

[1] M.C. Gonzalez-Garcia, M. Maltoni, *Phys. Rep.* **460**, 1 (2008).
[2] C. Giunti, M. Laveder, *Phys. Rev.* **C83**, 065504 (2011).
[3] C. Giunti *et al.*, `arXiv:1210.5715 [hep-ph]`.
[4] T.A. Mueller *et al.*, *Phys. Rev.* **C83**, 054615 (2011).
[5] G. Mention *et al.*, *Phys. Rev.* **D83**, 073006 (2011).
[6] P. Huber, *Phys. Rev.* **C84**, 024617 (2011).
[7] J.N. Bahcall, *Phys. Rev.* **C56**, 3391 (1997).
[8] D. Krofcheck *et al.*, *Phys. Rev. Lett.* **55**, 1051 (1985).
[9] W.C. Haxton, *Phys. Lett.* **B431**, 110 (1998).
[10] D. Frekers *et al.*, *Phys. Lett.* **B706**, 134 (2011).
[11] W. Hampel, L. Remsberg, *Phys. Rev.* **C31**, 666 (1985).
[12] K.N. Abazajian *et al.*, `arXiv:1204.5379 [hep-ph]`.
[13] C. Giunti, M. Laveder, *Phys. Lett.* **B706**, 200 (2011).
[14] C. Giunti, M. Laveder, Y. Li, H. Long, `arXiv:1212.3805 [hep-ph]`.